

- Cintala MJ, Wood CA, Head JW (1977) The effects of target characteristics on fresh crater morphology: preliminary results for the Moon and Mercury. *Proc 8th Lunar Sci Conf, Geochim Cosmochim Acta Suppl* 8:3409–3425 Houston, TX
- Florensky CP, Basilevsky AT, Grebennik NN (1976) The relationship between lunar crater morphology and crater size. *Moon* 16:59–70
- Howard KA (1974) Fresh lunar impact craters: review of variation with size. *Proc 5th Lunar Sci Conf, Geochim Cosmochim Acta Suppl* 5(1):61–69
- Pike RJ (1974) Depth/diameter relations of fresh lunar craters: revision from spacecraft data. *Geophys Res Lett* 1:291–294
- Pike RJ (1977a) Apparent depth/diameter relations for lunar crater. *Proc 8th Lunar Sci Conf, Geochim Cosmochim Acta Suppl* 8:3427–3436
- Pike RJ (1977b) Size dependence in the shape of fresh impact craters on the Moon. In: Roddy DJ et al (eds) *Impact and explosion cratering*. Pergamon Press, New York, pp 489–509
- Pike RJ (1988) Geomorphology of impact craters on Mercury. In: Vilas F, Chapman CR, Matthews MS (eds) *Mercury*. University of Arizona Press, Tucson, pp 165–273
- Robbins SJ, Hynek BM (2012) A new global database of Mars impact craters ≥ 1 km: 1. Database creation, properties, and parameters. *J Geophys Res* 117, E05004
- Smith EJ, Sanchez AG (1973) Fresh lunar craters: morphology as a function of diameter, a possible criterion for crater origin. *Mod Geol* 4:51–59
- Smith EI, Hartnell, JA (1978) Crater size-shape profiles for the Moon and Mercury: Terrain effects and interplanetary comparisons. *Moon and te Planets* 19: 479–511.
- Wood CA, Anderson L (1978) New morphometric data for fresh lunar craters. *Proc 9th Lunar Planet Sci Conf, Geochim Cosmochim Acta Suppl* 10:3669–2689
- Young RA (1977) A stratigraphic model for Bessel crater and southern Mare Serenitatis. In: Roddy DJ et al (eds) *Impact and explosion cratering*. Pergamon Press, New York, pp 527–538

Transitional Ejecta

- [Combination Ejecta](#)

Transverse Aeolian Ridge (TAR)

Sharon A. Wilson
 Center for Earth and Planetary Studies,
 Smithsonian Institution, National Air and Space
 Museum, Washington, DC, USA

Definition

About 10-m-scale, light- or medium-toned albedo relative to surrounding terrain, ripple-like aeolian bedform on Mars.

Category

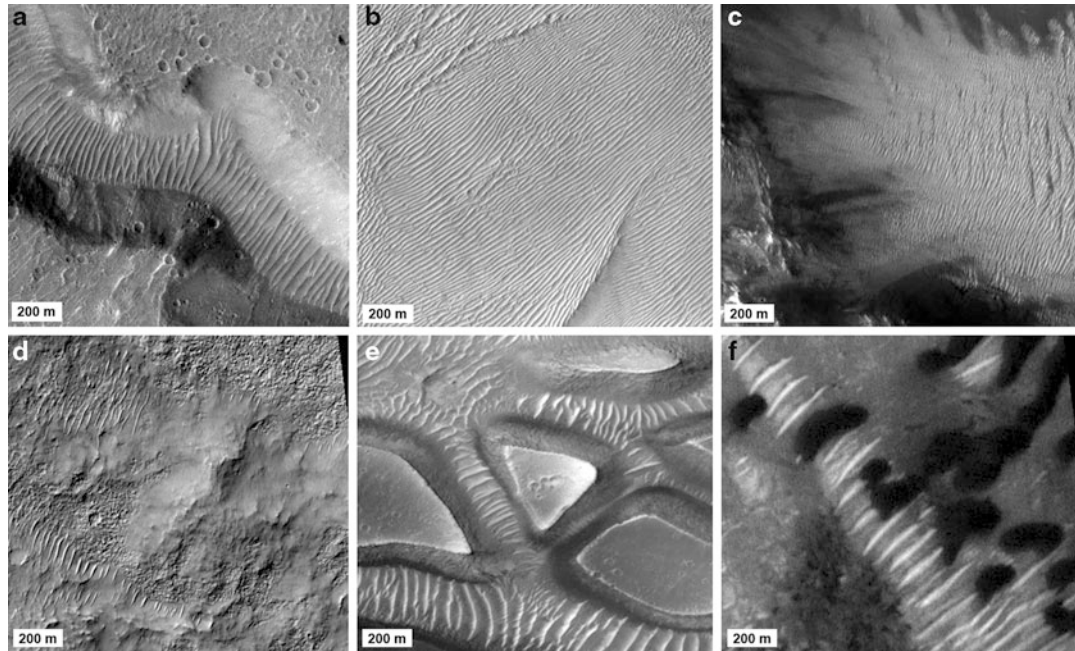
A type of ► [transverse dune](#) or transverse ripple (both are still viable options for formation).

Synonyms

Bright dunes (Edgett and Parker 1998; Malin et al. 1998; Thomas et al. 1999); Duneforms (e.g., Greeley et al. 2000; Fenton et al. 2003); Light-toned (linear) bedforms (Sullivan et al. 2008); Ripple band (Zimbelman and Wilson 2002); Ripple-like bedforms

Description

Transverse aeolian ridge (TAR), termed by Bourke et al. (2003), describes linear to curvilinear bedforms on Mars that formed as either large ripples or small dunes. These bedforms are morphologically distinct from ► [large dark dunes](#) (Fig. 1f). TARs are an order of magnitude smaller (decameter scale) than large dark dunes, generally brighter or the same relative albedo as the surrounding terrain (Malin and Edgett 2001) and lack observable slip faces (Bourke et al. 2003). Their simple form has nearly symmetrical crests (Malin and Edgett 2001; Bourke et al. 2006; Zimbelman 2010) that likely form transverse to local winds (Bourke et al. 2010).



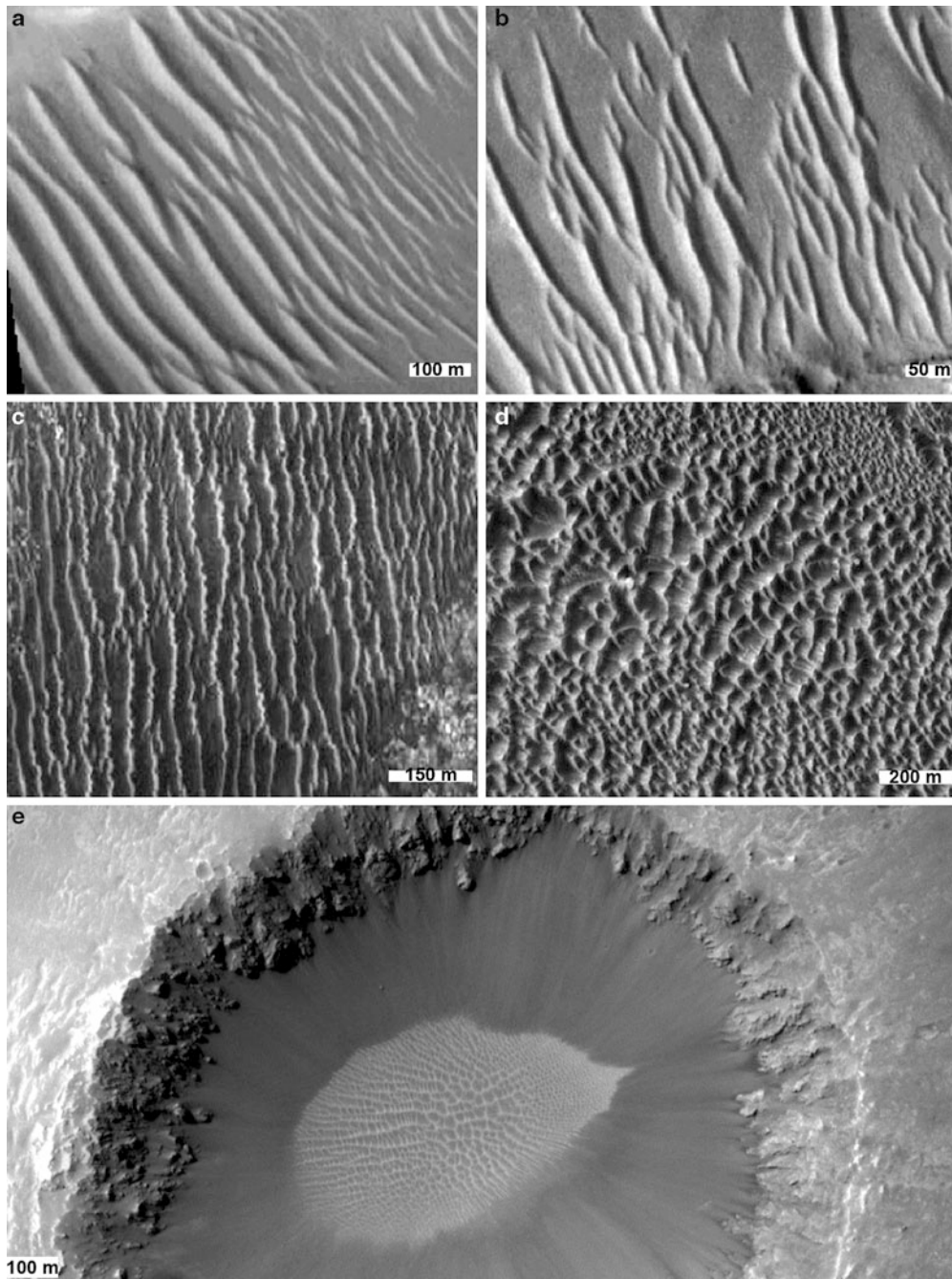
Transverse Aeolian Ridge (TAR), Fig. 1 Classification scheme for TARs on Mars by Wilson and Zimbelman (2004) based on the degree of topographic control, size of TAR deposit, and associations with other bedforms. (a) “Ripple bands” are topographically confined and develop in depressions such as troughs, valleys, and grabens. Crests are oriented perpendicular to the walls, presumably forming transverse to the local wind direction (MOC E10-02335 Nirgal Vallis); (b) TARs occur on larger flat-lying surfaces such as crater floors or plains as extensive

“ripple fields” (MOC E03-02283, Candor Chasma); (c) “large ripple patches” (MOC M04-02904, Syrtis/Isidis), or (d) “isolated ripple patches” (MOC M00-02082, southern highlands); (e) “obstacle ripples” (MOC E04-01514, Candor Chasma) occur around the bases of positive topographic features such as knobs, yardangs, and dunes; (f) occasionally, “dunes and ripples” occur together (MOC SP1-26004, crater floor), most commonly in intercrater dark dune fields in the southern hemisphere (Berman et al. 2011) (NASA/JPL/MSSS)

Subtypes

TARs exhibit a range of morphologies and their orientations and accumulations can be influenced by proximity to positive (e.g., mounds, dunes) or negative (e.g., crater, graben, or valley floors) topography. Wilson and Zimbelman (2004) described TARs in a classification scheme that combined level of (1) *topographic control* (ripple band and obstacle ripples), (2) *size* of TAR accumulation (ripple field, ripple patch, isolated ripple patches), and (3) *associations with other bedforms* (where TARs occur with dark dunes) (Fig. 1). Bourke et al. (2003) used a plan view shape to classify TARs within troughs as simple, sinuous, forked, feathered, and networked (Fig. 2).

Balme et al. (2008) combined and expanded these schemes and classified TARs based on (1) *morphology of the ridge crests* (simple, sinuous, formed, networked, and barchan-like, Fig. 2); (2) *degree of topographic control* (Fig. 3), (2.1) *confined* (located within a closed topographic depression (topographic trap), e.g., intracrater), (2.2) *controlled* (e.g., in an open depression or valley or adjacent to a local topographic high, e.g., mesa), (2.3) *influenced* (the overall distribution is not controlled by topography, but orientations of individual bedforms are influenced by topography, e.g., radial dunes/ripples around a mesa), and (2.4) *independent* (not influenced by local topography; e.g., in a flat plain); and (3) *size* of TAR accumulation (patches, fields, and seas have on the order of

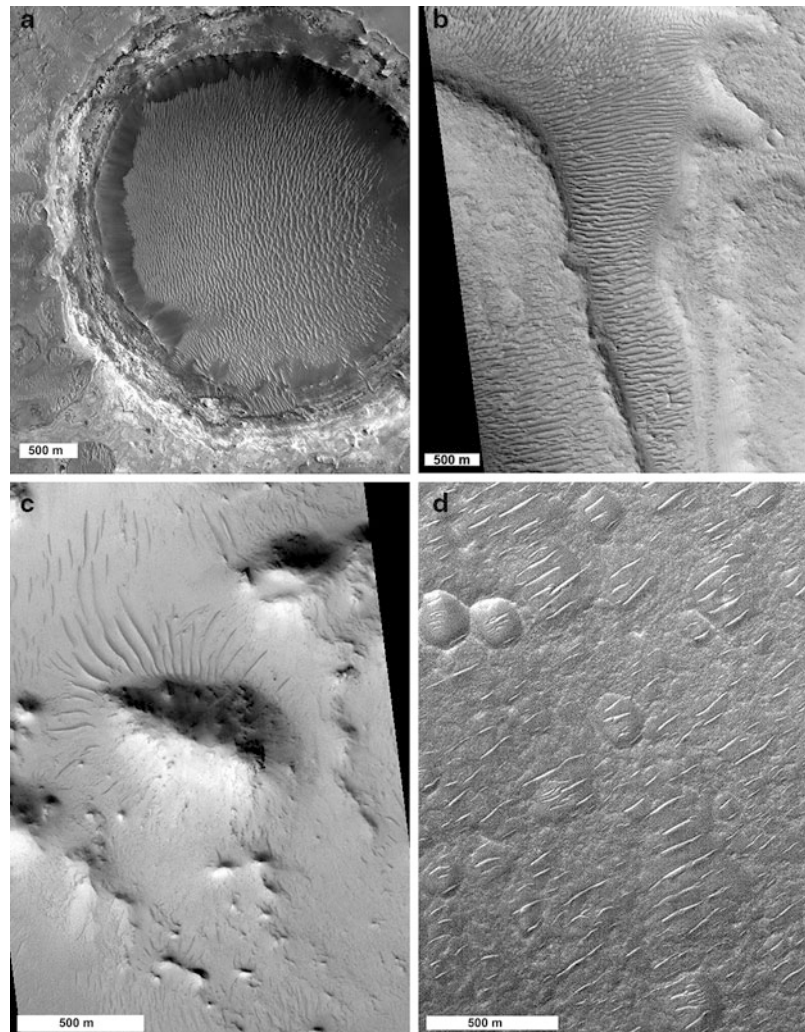


Transverse Aeolian Ridge (TAR), Fig. 2 TAR crest-ridge morphologies (Bourke et al. 2003; Balme et al. 2008). (a) “Simple”, at $\sim 21.3^\circ\text{N}$, 39.3°E (MOC M1104208); (b) *forked* (preferentially located at trough margins or adjacent to obstacles), at $\sim 20.7^\circ\text{N}$, 41.3°E (MOC M0303703); (c) *sinuous* (gently or tightly sinuous ridge crest), at $\sim 45.5^\circ\text{S}$, 28.7°E (MOC R0802177); (d) *barchan-like*, at $\sim 0.2^\circ\text{N}$, 0.1°E (MOC M1800277); and

(e) *networked* (form in local topographic depressions and areas of secondary flow circulation), at $\sim 0.1^\circ\text{S}$, 5.3°E (MOC R2300801). *Feathered* TARs, with small secondary ridges intersecting with or extending from the larger ridge (Bourke et al. 2003), are interpreted as secondary crests superposed on the primary bedforms and are therefore not included as a primary class by Balme et al. (2008) (NASA/JPL/MSSS)

Transverse Aeolian Ridge (TAR),

Fig. 3 Classification of TAR deposits by level of topographic control (Balme et al. 2008). (a) “Confined”, at $\sim 0.4^\circ\text{N}$, 5.4°E (MOC S0100833); (b) controlled, at $\sim 25.9^\circ\text{N}$, 10.4°E (MOC E1601902); (c) influenced, at $\sim 23.2^\circ\text{N}$, 7.2°E (MOC M1200437); and (d) independent, at $\sim 42.7^\circ\text{N}$, 43.9°E (MOC M1003676. NASA/JPL/MSSS)



tens, hundreds, and thousands of TARs or areas $>50 \text{ km}^2$, respectively).

Morphometry

The morphometry of TARs can be described by the crest-ridge width W , length L , and crest-to-crest wavelength or spacing λ (Balme et al. 2008, Fig. 4). Wilson and Zimbelman (2004) reported mean crest widths of 215 m (± 155 m) and average wavelengths of 40 m (typical range of 10–60 m) from over 340 measurements of TARs in MOC NA images (maximum 1.5 m/pixel). They noted little to no correlation between

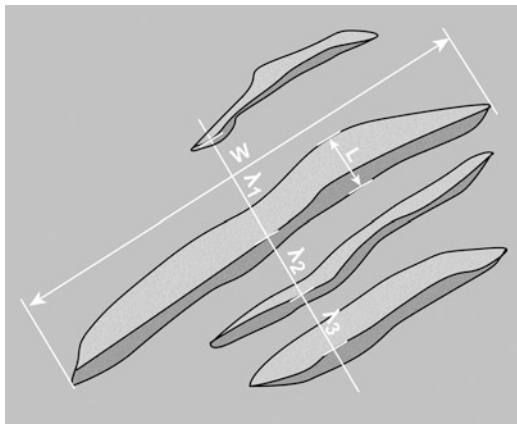
wavelength and crest length, although Bourke et al. (2003) noted that in TAR inter-bedform spacing (s , where $s = \lambda/L$), TARs seem more closely spaced in the narrowest parts of troughs and valleys. Zimbelman (2010) reported similar wavelengths using HiRISE data (average 37 m, range 7–70 m), and Balme et al. (2008) have identified wavelengths as small as 2.5 m in HiRISE images (25 cm/pixel). Balme et al. (2008) quantified variations in TAR spacing as saturated ($s = 1$), closely spaced (s is ~ 2 –3), and widely spaced ($s > 5$) (Fig. 5). The plan view aspect ratio a (where $a = W/L$) of TARs is generally > 6 but can range from ~ 2 to 15 (Balme et al. 2008).

Photoclinometric profiles of TARs from HiRISE data in Ius Chasma and Terra Sirenum revealed remarkably symmetric cross-sectional profiles with average slopes of $\sim 15^\circ$ for the entire feature (Zimbleman 2010). Height estimates of TARs using varying techniques including shadow measurements, stereo images, photoclinometry, and extrapolation of terrestrial examples range from roughly 1 to 8 m (Zimbleman 2000; Williams et al. 2003; Bourke

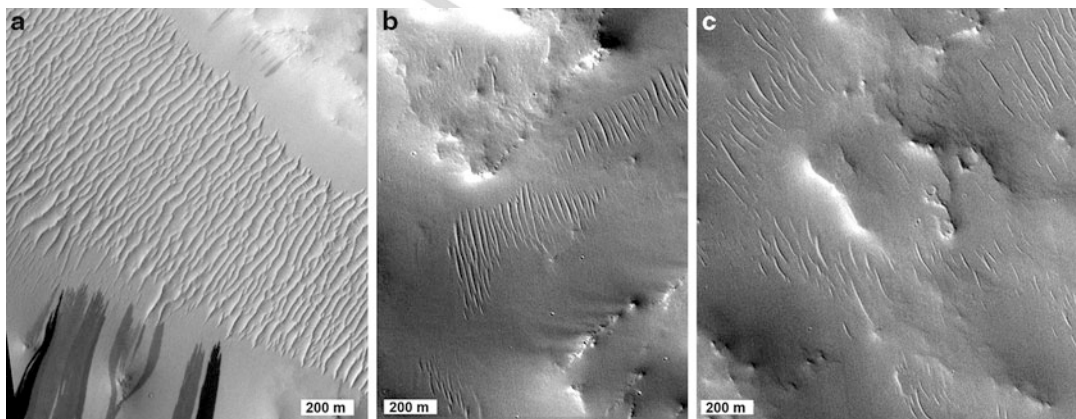
et al. 2006; Wilson et al. 2003; Zimbleman et al. 2012) (Figs. 6, 7).

Interpretation

TARs are widely believed to be a unique class of geologically young aeolian bedforms on Mars that formed as either transverse dunes or granule ripples. The simple, narrow, and transverse nature of TARs is analogous to large terrestrial ripples (Williams et al. 2002; Zimbleman and Wilson 2002; Wilson et al. 2003) such as “aeolian ridges” (Bagnold 1941), “granule ripples” (Sharp 1963; Fryberger et al. 1992), or “megaripples” (Greeley and Iversen 1985). On Earth, transverse dunes and granule ripples are characterized by differences in scale, morphology, and texture. Transverse dunes are generally well-sorted, large wavelength deposits with slip faces and superposed bedforms. Granule ripples are smaller deposits that lack slip faces and consist of sand or granules at the surface and fine-grained, poorly sorted material within (Wilson 1972). Some TARs might be bedrock ridges eroded into cohesive substrate rather than aeolian deposits (Montgomery et al. 2012).

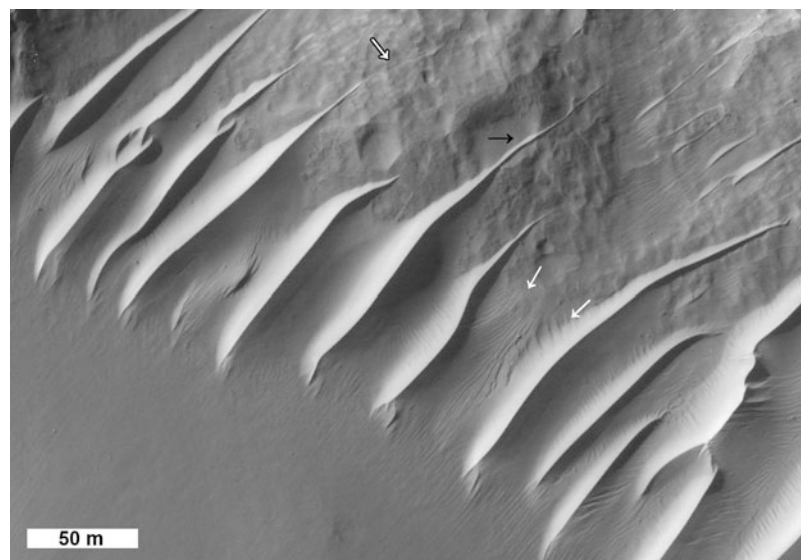


Transverse Aeolian Ridge (TAR), Fig. 4 Morphometric parameters used to describe TARs (After Balme et al. 2008)



Transverse Aeolian Ridge (TAR), Fig. 5 Range of TAR spacing (Balme et al. 2008). (a) Saturated TARs with $s \sim 1$ (near 0.1°N , 37.8°E , MOC R0400111); (b) medium inter-bedform spacing with $s \sim 2\text{--}3$ (near 24°N ,

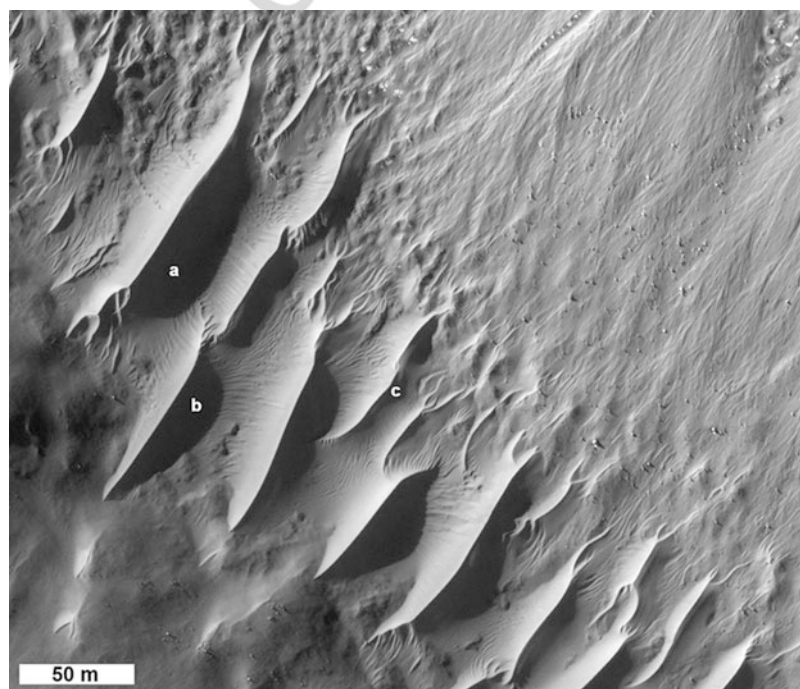
34.3°E , MOC M0705509); and (c) unsaturated or widely spaced TARs with $s > 5$ (near 19.5°N , 35.3°E , MOC M0900169. NASA/JPL/MSSS)



Transverse Aeolian Ridge (TAR), Fig. 6 TARs in Terra Sirenum. TARs taper to very thin linear ridges extending from their northern ends (*black arrow*), some of which separate into isolated linear segments following the trend of the nearby TAR (*white arrow with a black outline*). The narrow extensions suggest erosion of

inactive TARs rather than extension of active TARs along such narrow bands. Subtle aeolian bedforms are visible both between and on the TARs (*white arrows*) (After Zimbelman 2010. HiRISE PSP_001684_1410, 38.9°S, 196.0°E. NASA/JPL/U of A)

Transverse Aeolian Ridge (TAR), Fig. 7 Forked terminations of Terra Sirenum TAR crests, along with evidence of eroded layers exposed both in the interdune regions and even on the slopes of some TARs. The low solar incidence angle (16°) casts long shadows that provide heights for several TARs (*a* 8.03 m, *b* 5.73 m, *c* 2.29 m). Gully deposits are visible on the *upper right* (After Zimbelman 2010. HiRISE PSP_001684_1410 NASA/JPL/U of A)



Formation

Morphologic analyses of TARs using HiRISE images suggest a transverse dune origin for TARs with heights ≥ 1 m, whereas TARs ≤ 0.5 m in height are likely granule ripples (Zimbelman 2010). TARs with larger wavelengths (>15 m) may be reversing dunes, whereas smaller wavelength TARs (3–15 m) may be analogous to granule ripples (Zimbelman 2008). Alternatively, these enigmatic bedforms may represent the transition between large granule ripples and small aeolian dunes (Williams et al. 2002; Zimbelman and Wilson 2002; Wilson et al. 2003; Balme et al. 2008). At least some TARs may be granule ripples based on the observation that they appear active when associated with large dune fields that provide a constant supply of saltating material, and TARs distal to large dunes under present-day atmospheric conditions are likely not active (Berman et al. 2011).

Degradation

TARs are relatively undegraded bedforms. The age of TARs has been estimated by conducting crater count analyses from MOC NA (Reiss et al. 2004) and HiRISE (Berman et al. 2011) images. Reiss et al. reported TARs in Nirgal Vallis ceased to be active 1.4–0.3 Ma before present. Berman et al. found that equatorial TARs in Meridiani are ~ 1 –3 Ma old compared to southern highland TARs that lack craters >5 –10 m in diameter and therefore are likely formed less than 100 ka years ago. In many cases, large dark dunes migrating across TARs (Fig. 1f) leave them unaltered, suggesting TARs are indurated or lithified (Wilson and Zimbelman 2004; Balme et al. 2008). Extremely narrow extensions of some TARs (Fig. 6) suggest these bedforms are inactive and eroding (Zimbelman 2010).

Composition

The composition and particle size of TARs remains uncertain (Wilson and Zimbelman 2004), but they likely formed from local sediment sources (Fenton et al. 2003) as inferred by their common association with nearby layered terrains and steep slopes (Balme et al. 2008). Thermal inertia values of TARs from THEMIS data indicate TARs have lower thermal values relative to the large dark dunes (Zimbelman 2003; Balme and Bourke 2005; Fenton and Mellon 2006). If the mineralogy of TARs and dark dunes are the same, the lower thermal signature of TARs indicates (1) TARs consist of smaller grains, (2) grain sizes are comparable but the dark dunes are lithified, or (3) particle sizes are comparable but the particles making up the TARs may have intrinsically lower thermal particles (e.g., porous, agglomerates, etc.) (Balme et al. 2008). In Nirgal Vallis, the thermal signature of TARs is consistent with moderate to coarse sand (Zimbelman 2003). Studies have proposed compositions including relatively soft materials such as gypsum or other sulfates (Thomas et al. 1999), quartz or feldspar, and evaporates and (or) carbonates (Edgett and Parker 1998).

Distribution

Pole-to-pole surveys on opposite sides of the planet between 180°E and 240°E (Wilson and Zimbelman 2004) and ~ 0 and 45°E (Balme et al. 2008; Berman et al. 2011) indicate TARs are concentrated in the mid to low latitudes of both hemispheres. The survey by Berman et al. (2011) estimates 5 % of the surface is covered by TARs with concentrations around the equator and large craters in the southern highlands. Although TARs have been found on the Tharsis volcanoes (Malin and Edgett 2001), they are less common at extreme elevations (Wilson and Zimbelman 2004; Berman et al. 2011). Local geology controls the distribution of TARs (Wilson and Zimbelman 2004; Berman et al. 2011), their orientation matches present-day regional wind patterns (Berman et al. 2011),

and there is no apparent correlation with thermal inertia (Wilson and Zimbelman 2004).

Significance

TARs are widespread aeolian bedforms on Mars, but the formation mechanism, age, composition, and factors controlling their distribution and role in the global sediment cycle are poorly constrained.

Terrestrial Analog

small dunes, aeolian ridges, granule ripples (megaripples).

Origin of Term

They were first noted in images from the Viking orbiter (Zimbelman 1987; Edgett and Parker 1998) and more recently in narrow angle (NA) images from the Mars Orbiter Camera (Thomas et al. 1999; Malin and Edgett 2001). TARs were named by Bourke et al. (2003) to preserve ripple or dune options for their unknown origin.

Similar Landforms Derived from Different Processes

- Periodic bedrock ridge (Mars)

See Also

- Dune
- Large Dark Dune
- Megaripple
- Ripple
- Transverse Ridge

References

- Bagnold RA (1941) The physics of brown sand and desert dunes. Methuen, London
- Balme MR, Bourke MC (2005) Preliminary results from a new study of transverse aeolian ridges (TARs) on Mars. Lunar Planet Sci Conf XXXVI, abstract #1892, League City, Texas, March 14–18
- Balme M, Berman DC, Bourke MC, Zimbelman J (2008) Transverse aeolian ridges (TARs) on Mars. *Geomorphology* 101:703–720
- Berman DC, Balme MR, Rafkin SCR, Zimbelman JR (2011) Transverse aeolian ridges (TARs) on Mars II: distributions, orientations, and ages. *Icarus* 213:116–130
- Bourke MC, Wilson SA, Zimbelman JR (2003) The variability of TARs in troughs on Mars. Lunar Planet Sci Conf XXXIV, abstract #2090, League City, Texas, March 17–21
- Bourke MC, Balme MR, Beyer RA, Williams KK, Zimbelman J (2006) A comparison of methods used to estimate the height of sand dunes on Mars. *Geomorphology* 81(3–4):440–452
- Bourke MC, Lancaster N, Fenton LK, Parteli EJR, Zimbelman JR, Radebaugh J (2010) Extraterrestrial dunes: an introduction to the special issue on planetary dune systems. *Geomorphology* 121:1–14
- Edgett KS, Parker TJ (1998) “Bright” aeolian dunes on Mars: Viking Orbiter observations. Lunar Planet Sci Conf XXIX, abstract #1338, Houston, March 16–20
- Fenton LK, Mellon MT (2006) Thermal properties of sand from Thermal Emission Spectrometer (TES) and Thermal Emission Imaging System (THEMIS): spatial variations within the Proctor Crater dune field on Mars. *J Geophys Res* 111 (E06). doi: 10.1029/2004JE002363
- Fenton LK, Bandfield JL, Ward AW (2003) Aeolian processes in Proctor Crater on Mars: sedimentary history as analyzed from multiple data sets. *J Geophys Res* 108(E12):5129. doi:10.1029/2002JE002015
- Fryberger SG, Hesp P, Hastings K (1992) Aeolian granule ripple deposits in Namibia. *Sedimentology* 39:319–331
- Greeley R, Iversen JD (1985) Wind as a geological process on Earth, Mars, Venus and Titan. Cambridge University Press, Cambridge
- Greeley R, Kraft MD, Kuzmin RO, Bridges NT (2000) Mars Pathfinder landing site: evidence for a change in wind regime from lander and orbiter data. *J Geophys Res* 105:1829–1840
- Malin MC, Edgett KS (2001) Mars global surveyor Mars orbiter camera: interplanetary cruise through primary mission. *J Geophys Res* 106:23,429–23,570
- Malin MC et al (1998) Early views of the Martian surface from the Mars Orbiter Camera of Mars Global Surveyor. *Science* 279:1681–1685
- Montgomery DR, Bandfield JL, Becker SK (2012) Periodic bedrock ridges on Mars. *J Geophys Res* 117: E03005. doi:10.1029/2011JE003970

- Reiss D, van Gasselt S, Neukum G, Jaumann R (2004) Absolute dune ages and implications for the time of formation of gullies in Nirgal Vallis, Mars. *J Geophys Res* 109(E06). doi:10.1029/2004JE002251
- Sharp RP (1963) Wind ripples. *J Geol* 71:617–636
- Sullivan R, Arvidson R, Bell JF, Gellert R, Golombek M, Greeley R, Herkenhoff K, Johnson J, Thompson S, Whelley P, Wray J (2008) Wind-driven particle mobility on Mars: insights from Mars Exploration Rover observations at “El Dorado” and surroundings at Gusev Crater. *J Geophys Res* 113:E6. doi:10.1029/2008JE003101
- Thomas PC, Malin MC, Carr MH, Danielson GE, Davies ME, Hartmann WK, Ingersoll AP, James PB, McEwen AS, Soderblom LA, Veverka J (1999) Bright dunes on Mars. *Nature* 397:592–594. doi:10.1038/17557
- Williams SH, Zimbelman JR, Ward AW (2002) Large ripples on Earth and Mars. *Lunar Planet Sci Conf XXXIII*, abstract #1508, League City, March 11–15
- Williams KK, Greeley R, Zimbelman JR (2003) Using overlapping MOC images to search for dune movement and to measure dune height. *Lunar Planet Sci Conf XXXIV*, abstract #1639 League City, March 17–21
- Wilson IG (1972) Aeolian bedforms: their development and origins. *Sedimentology* 19:173–210
- Wilson SA, Zimbelman JR (2004) Latitude-dependent nature and physical characteristics of transverse aeolian ridges on Mars. *J Geophys Res* 109, E10003. doi:10.1029/2004JE002247
- Wilson SA, Zimbelman JR, Williams SH (2003) Large aeolian ripples: extrapolations from Earth to Mars. *Lunar Planet Sci Conf XXXIV*, abstract #1862 League City, March 17–21
- Zimbelman JR (1987) Spatial resolution and the geologic interpretation of Martian morphology: implications for subsurface volatiles. *Icarus* 74:257–267
- Zimbleman JR (2000) Non-active dunes in the Acheron Fossae region of Mars between the Viking and Mars Global Surveyor eras. *Geophys Res Lett* 27(7):1069–1072
- Zimbelman JR (2003) Decameter-scale ripple-like features in Nirgal Vallis as revealed in THEMIS and MOC imaging data. In: Sixth international conference on Mars, Pasadena, July 20–25 #3028
- Zimbelman JR (2008) An MRO view of transverse aeolian ridges on Mars. In: American Geophysical Union, Fall meeting 2008, San Francisco, California, Dec 15–19 #P41B-1369
- Zimbelman JR (2010) Transverse aeolian ridges on Mars: first results from HiRISE images. *Geomorphology* 121:22–29
- Zimbelman JR, Wilson S (2002) Ripples and dunes in the Syrtis Major region of Mars, as revealed in MOC images. *Lunar Planet Sci Conf XXXIII*, abstract #1514 League City, March 11–15
- Zimbelman JR, Williams SH, and Johnston AK (2012) Cross-sectional profiles of sand ripples, megaripples, and dunes: A method for discriminating between formational mechanisms. *Earth Surf. Proc. Landforms* 37; 1120–1125, doi: 10.1002/esp.3243

Transverse Dune

► Transverse Ridge

Transverse Dunes

Kathryn E. Fitzsimmons
Department of Human Evolution, Max Planck
Institute for Evolutionary Anthropology,
Leipzig, Germany

Definition

Aeolian deposits where the longest axis forms perpendicular to the resultant wind or sand-transport direction, broadly linear or crescentic in form. Transverse dunes can also be defined as dunes characterized by slipfaces in one direction, representing unidirectional wind regime (McKee 1979, p. 9). The term *transverse* in this sense can be used without strict regard to dune orientation.

Subtypes in the order of decreasing available sand supply:

Drifting sand (McKee 1979, p. 9):

- (1) ► **Transverse ridges** (parallel straight ridges)
- (2) ► **Barchanoid ridges** (parallel rows of coalesced barchans)
- (3) ► **Barchans** (isolated crescentic transverse dunes)

They may occur in gradational sequence downwind as a result of diminishing sand supply (Fig. 1)